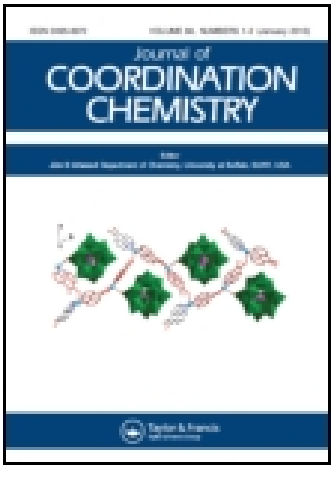

Journal of Coordination Chemistry
Publication details, including instructions for authors and subscription information:
http://www.tandfonline.com/loi/gcoo20

Synthesis, properties, and X-ray crystal structures of two Ag(I) complexes with 2-(pyridin-4-yl)-1H-imidazole-4,5-dicarboxylic acid

Juan Zheng[a], Dan Zhou[a], Tan-Hao Shi[a], Qiao-Qiao Guan[a] & Yan Xu[a]
[a] The College of Chemistry and Molecular Engineering, Zhengzhou University, Zhengzhou, PR China

Accepted author version posted online: 11 Feb 2014.Published online: 24 Feb 2014.

To cite this article: Juan Zheng, Dan Zhou, Tan-Hao Shi, Qiao-Qiao Guan & Yan Xu (2014) Synthesis, properties, and X-ray crystal structures of two Ag(I) complexes with 2-(pyridin-4-yl)-1H-imidazole-4,5-dicarboxylic acid, Journal of Coordination Chemistry, 67:3, 533-544, DOI: 10.1080/00958972.2014.885508

To link to this article: http://dx.doi.org/10.1080/00958972.2014.885508

Journal of Coordination Chemistry, 2014
Vol. 67, No. 3, 533–544, http://dx.doi.org/10.1080/00958972.2014.885508

Synthesis, properties, and X-ray crystal structures of two Ag(I) complexes with 2-(pyridin-4-yl)-1*H*-imidazole-4,5-dicarboxylic acid

JUAN ZHENG, DAN ZHOU, TAN-HAO SHI, QIAO-QIAO GUAN and YAN XU*

The College of Chemistry and Molecular Engineering, Zhengzhou University, Zhengzhou, PR China

(*Received 4 August 2013; accepted 30 December 2013*)

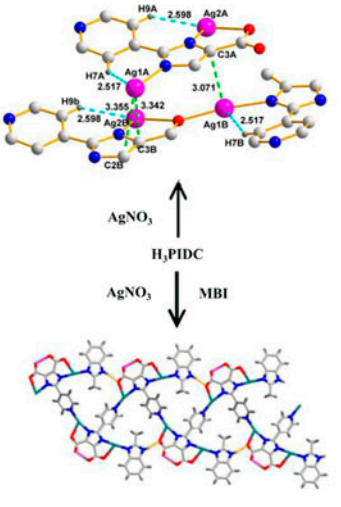

Two new complexes formulated as $[Ag_2(H_2PIDC)]_n$ (**1**) and $[Ag_2(HPIDC)(MBI)]_n$ (**2**) {H_3PIDC = 2-(pyridin-4-yl)-1*H*-imidazole-4,5-dicarboxylic acid, MBI = 2-methyl-1H-benzo[d]imidazole} have been synthesized and characterized by infrared spectroscopy, elemental analysis, and single-crystal X-ray diffraction. The most interesting structural features of these complexes are the presence of obvious C–H···Ag hydrogen bonding interactions and Ag···C weak interactions between the Ag centers and H_3PIDC ligands. In addition, their luminescent properties have been investigated in the solid state at room temperature.

Two 1-D and 3-D Ag(I) complexes involving 2-(pyridin-4-yl)-1*H*-imidazole-4,5-dicarboxylic acid (H_3PIDC) have been characterized by infrared spectrum, elemental analysis, and single-crystal X-ray diffraction. $[Ag_2(HPIDC)]_n$ (**1**), synthesized under hydrothermal conditions, gave a 3-D framework; $[Ag_2(HPIDC)(MBI)]_n$ (**2**) (MBI = 2-methyl-1*H*-benzo[*d*]imidazole), with MBI as the second ligand, gave a 1-D zigzag chain and further formed a 3-D supramolecular structure through

*Corresponding author. Email: xuyan@zzu.edu.cn

$\pi\cdots\pi$ interactions. The most interesting structural features of these complexes are the presence of C–H···Ag hydrogen bonding interactions and Ag···C weak interactions between the Ag centers and H_3PIDC. Luminescence indicates that **2** has significantly stronger fluorescent emissions than **1** in the solid state at room temperature.

Keywords: 2-(Pyridin-4-yl)-1*H*-imidazole-4,5-dicarboxylic acid; Ag(I) complexes; Crystal structure; Luminescence

1. Introduction

The design and synthesis of metal-organic frameworks (MOFs) have provoked significant interest, owing to their variety of intriguing structural topologies as well as potential applications as microporous, magnetic, non-linear optical, and fluorescent materials [1]. Selection of aromatic polycarboxylates as multifunctional ligands is an effective approach to construct MOFs with unique structures and properties [2]. Increasing interest has concentrated on rigid *N*-heterocyclic multi-carboxylates due to their diversities in coordination modes and conformations according to the restrictions imposed by the coordination geometry of the metal ion [3–5]. 2-(Pyridin-4-yl)-1*H*-imidazole-4,5-dicarboxylic acid (H_3PIDC), as a multidentate rigid ligand, which can be μ-2, μ-3, and μ-4 to generate MOFs, and pyridyl group to give more potential coordination modes with rotation around the C–C bond to meet coordination requirements of metal ions in assembly, has interesting traits in construction of MOFs [6]. H_3PIDC with three hydrogens can be deprotonated to form H_2PIDC^-, $HPIDC^{2-}$, and $PIDC^{3-}$, and enlarge the conjugated π-system, resulting in diverse supramolecular architectures [7]. A number of complexes with H_3PIDC have been reported [8], but as the central metal ion, silver is a particularly versatile transition metal in its coordination number and arrangement [9–13]. Ag(I) usually exhibits a variety of coordination geometries such as linear, trigonal planar, T-shaped, tetrahedral, etc. When Ag(I) coordinates to appropriate ligands, complexes show a variety of configurations, 1-D, 2-D, and 3-D structures [14–19]. For Ag(I) complexes with aromatic ligands, not only $\pi\cdots\pi$ stacking interactions between aromatic rings form, but also Ag$\cdots\pi$ and C–H···Ag close interactions appear [20, 21]. These interactions are important in formation of multi-dimensional Ag(I) coordination supramolecules. The semirigid 2-methyl-1*H*-benzo[*d*]imidazole (MBI) with two N-donors can adopt different conformation to coordinate with metal ions, beneficial to construct extended architectures. Furthermore, the methyl substituent in the 2-position of the benzimidazole ring can enhance electron-donating ability of the ligand [22, 23]. Research of Ag(I) complexes with H_3PIDC remains unexplored. Herein, we report the synthesis, structural characterizations, fluorescence properties, and thermogravimetric analysis of two silver-based complexes with 1-D and 3-D frameworks and present the C–H···Ag, Ag···C close interactions for the first time in silver(I)–H_3PIDC complexes.

2. Experimental

The ligand H_3PIDC was synthesized according to the literature method [24]. All reagents and solvents employed were of AR Grade from commercial sources and used as received. IR data were recorded on a BRUKER TENSOR 27 spectrophotometer with KBr pellets from 400 to 4000 cm^{-1}. Elemental analyses (C, H, and N) were carried out on a FLASH EA 1112 elemental analyzer. Steady state fluorescence measurements were performed on a

Fluoro Max-P spectrofluorimeter at room temperature with solid powder on a 1 cm quartz round plate. The excitation slit and the emission slit were 5 nm; the response time was 2 s. Thermogravimetric analyses (TGA) of the samples were performed using a Perkin-Elmer TG-7 analyzer heated from room temperature to 1000 °C under nitrogen.

2.1. *Synthesis of $[Ag_2(HPIDC)]_n$ (1)*

A mixture of $AgNO_3$ (0.100 mM, 0.0170 g) and H_3PIDC (0.100 mM, 0.0233 g) in CH_3CN–H_2O mixed solvent (10 mL, v/v, 7 : 3) was placed in a Teflon reactor (25 mL) and heated at 170 °C for three days and subsequently cooled to room temperature at 5 °C h^{-1}. Faint-yellow transparent crystals of **1** were obtained. Anal. Calcd for $C_{10}H_5Ag_2N_3O_4$ (%): C, 26.92; H, 1.10; N, 9.42. Found: C, 26.87; H, 1.13; N, 9.40. IR (KBr, cm^{-1}): 3426(m), 1667(m), 1612(s), 1530(s), 1436(s), 1360(s), 1293(m), 1255(m), 1219(m), 1036(m), 833(s), 775(m), 741(m), 707(m), 667(w), 550(m), 520(m), 460(w).

2.2. *Synthesis of $[Ag_2(HPIDC)(MBI)]_n$ (2)*

A mixture of $AgNO_3$ (0.100 mM, 0.0170 g), H_3PIDC (0.100 mM, 0.0233 g), and MBI (0.100 mM, 0.0132 g) in CH_3CN–H_2O mixed solvent (10 mL, v/v, 7 : 3) was placed in a Teflon reactor (25 mL) and heated at 170 °C for three days and subsequently cooled to room temperature at 5 °C h^{-1}. Light-yellow crystals of **2** were obtained. Anal. Calcd for $C_{18}H_{13}Ag_2N_5O_4$ (%): C, 37.43; H, 2.28; N, 12.18. Found: C, 37.33; H, 2.26; N, 12.09. IR (KBr, cm^{-1}): 3420(w), 2970(w), 2921(w), 1682(m), 1612(m), 1574(s), 1458(s), 1364(s), 1268(m), 1219(m), 1122(m), 1002(m), 855(m), 835(m), 766(m), 714(m), 626(m), 541(m).

Table 1. Crystal data and structural refinement parameters of **1** and **2**.

Complexes	**1**	**2**
Empirical formula	$C_{10}H_5Ag_2N_3O_4$	$C_{18}H_{13}Ag_2N_5O_4$
Formula weight	446.91	579.07
Temperature (K)	291(2)	291.15
Crystal system	Monoclinic	Monoclinic
Space group	*Cc*	$P2_1/c$
a (Å)	5.2081(10)	6.7379(5)
b (Å)	20.1881(4)	13.1402(8)
c (Å)	10.4953(2)	20.9377(16)
α (°)	90.00	90.00
β (°)	101.180(2)	106.413(7)
γ (°)	90.00	90.00
Volume ($Å^3$)	1082.55(4)	1778.2(2)
Z	4	1
Calculated density (kg/m^3)	2.742	2.163
Absorption coefficient (mm^{-1})	3.631	2.241
F (0 0 0)	848	1128.0
Crystal sizes (mm)	0.20 × 0.14 × 0.12	0.12 × 0.08 × 0.08
R(int)	0.0218	0.0000
Data/restraints/parameters	1827/2/172	5754/0/264
Goodness-of-fit on F^2	1.023	1.037
Final *R* indices [$I > 2\sigma(I)$]	$R1 = 0.0179$, $wR2 = 0.0356$	$R1 = 0.0626$, $wR2 = 0.1783$
R indices (all data)	$R1 = 0.0189$, $wR2 = 0.0362$	$R1 = 0.0731$, $wR2 = 0.1$

2.3. *Single-crystal structure determination*

A suitable single crystal of each complex was carefully selected and glued to a thin glass fiber. Crystal structure determination by X-ray diffraction was performed on a Rigaku Saturn 724 CCD area detector with graphite monochromator for the X-ray source (MoKα radiation, $\lambda = 0.71073$ Å) operating at 50 kV and 40 mA. The crystal–detector distance was 45 mm. An empirical absorption correction was applied. The data were corrected for Lorentz–polarization effects. The structures were solved by direct methods and refined by full-matrix least-squares and difference Fourier techniques, based on F^2, using SHELXS-97 [25]. All non-hydrogen atoms were refined anisotropically. Hydrogens were positioned geometrically and refined using a riding model. All hydrogens were included in the final refinement. Crystallographic parameters and structural refinement data for the complexes are summarized in table 1. Selected bond lengths and angles are listed in table 2. Hydrogen bonds of **2** are listed in table 3.

Table 2. Selected bond distances (Å) and angles (°) for **1** and **2** with estimated standard deviations in parentheses.

Complex **1**			
Ag(1)–O(1)	2.566(3)	O(3)$^{\#1}$–Ag(1)–O(1)	117.06(10)
Ag(1)–O(3)$^{\#1}$	2.150(3)	O(3)$^{\#1}$–Ag(1)–N(1)	170.60(12)
Ag(1)–N(1)	2.161(3)	N(1)–Ag(1)–O(1)	71.95(11)
Ag(2)–O(3)	2.536(3)	N(2)–Ag(2)–O(3)	71.53(11)
Ag(2)–N(2)	2.139(3)	N(3)$^{\#2}$–Ag(2)–O(3)	118.00(12)
Ag(2)–N(3)$^{\#2}$	2.125(4)	N(3)$^{\#2}$–Ag(2)–N(2)	170.29(13)
O(3)–Ag(1)$^{\#3}$	2.150(2)	C(1)–O(1)–Ag(1)	108.6(3)
N(3)–Ag(2)$^{\#4}$	2.125(4)	Ag(1)$^{\#3}$–O(3)–Ag(2)	133.69(12)
C(4)–O(3)–Ag(1)$^{\#3}$	114.5(3)	C(4)–O(3)–Ag(2)	111.6(3)
C(2)–N(1)–Ag(1)	118.5(3)	C(5)–N(1)–Ag(1)	135.8(3)
C(3)–N(2)–Ag(2)	118.4(2)	C(5)–N(2)–Ag(2)	135.6(3)
C(6)–N(3)–Ag(2)$^{\#4}$	122.9(3)	C(10)–N(3)–Ag(2)$^{\#4}$	120.6(3)
Complex **2**			
Ag(1)–O(1)	2.553(6)	N(1)–Ag(1)–O(1)	72.42(19)
Ag(1)–N(1)	2.141(6)	N(3)$^{\#1}$–Ag(1)–O(1)	119.9(2)
Ag(1)–N(3)$^{\#1}$	2.136(6)	N(3)$^{\#1}$–Ag(1)–N(1)	167.6(2)
Ag(2)–N(2)	2.097(6)	N(4)–Ag(2)–N(2)	175.9(2)
Ag(2)–N(4)	2.077(6)	C(1)–O(1)–Ag(1)	109.0(5)
N(3)–Ag(1)$^{\#2}$	2.136(6)	C(2)–N(1)–Ag(1)	118.1(5)
C(5)–N(1)–Ag(1)	135.9(5)	C(3)–N(2)–Ag(2)	120.9(5)
C(5)–N(2)–Ag(2)	132.9(5)	C(6)–N(3)–Ag(1)$^{\#2}$	123.4(5)
C(10)–N(3)–Ag(1)$^{\#2}$	119.9(5)	C(16)–N(4)–Ag(2)	123.1(5)
C(17)–N(4)–Ag(2)	131.3(5)		

Symmetry transformations used to generate equivalent atoms: For **1**: $^{\#1}x-3/2, -y+1/2, z-1/2$; $^{\#2}x+1, -y+1, z+1/2$; $^{\#3}x+3/2, -y+1/2, z+1/2$; $^{\#4}x-1, -y+1, z-1/2$. For **2**: $^{\#1}2-x, -1/2+y, 3/2-z$; $^{\#2}2-x, 1/2+y, 3/2-z$.

Table 3. Data of hydrogen bond interactions (Å) of **2**.

D–H···A	*d*(D–H) (Å)	*d*(H···A) (Å)	*d*(D···A) (Å)	∠(DHA) (°)
N3–H3···O2	0.82	1.66	2.478(8)	170.7
N5–H5···O1$^{\#1}$	0.86	1.90	2.742(9)	166.2

Symmetry code: $^{\#1}+x, 1+y, +z$.

3. Results and discussion

3.1. *IR spectroscopy of ligand, 1 and 2*

IR spectra of **1** and **2** show a broadband at 3426 and 3420 cm^{-1} due to the active hydrogen of ligand, indicating active hydrogen group participating in the hydrogen bonding in **2** (the absorption of free ligand is at 3407 cm^{-1}). The bands at 3157 and 3072 cm^{-1} in free ligand can be ascribed to O–H stretch of –COOH, whereas the absence of these bands for **1** and **2** indicates deprotonation of –COOH to form COO^-. In **1**, Δv ($v_{as}COO–v_{sym}COO$) = 266 cm^{-1} indicates monodentate coordination [26] (v_{as}(COO) at 1666 cm^{-1} and v_{sym}(COO) at 1400 cm^{-1}) and $\Delta v = 50$ cm^{-1} indicates bidentate coordination (v_{as}(COO) at 1530 cm^{-1} and v_{sym}(COO) at 1480 cm^{-1}). For **2**, $\Delta v = 224$ cm^{-1} (v_{as}(COO) at 1682 cm^{-1} and v_{sym}(COO) at 1458 cm^{-1}) indicates monodentate coordination. The skeletal vibration absorptions of aromatic rings are at 1667–1436 cm^{-1} and 1682–1458 cm^{-1}.

3.2. *Structural description of $[Ag_2(HPIDC)]_n$*

X-ray single-crystal diffraction analysis reveals that **1** crystallizes in the space group *Cc* with a 3-D framework. The asymmetric unit of **1** contains two Ag(I) ions (Ag1 and Ag2) and one $HPIDC^{2-}$. As shown in figure 1(a), both Ag1 and Ag2 cations have slightly distorted trilateral environments. The coordinate geometry of Ag1 is completed by O1, O3, and N1 from two $HPIDC^{2-}$ ligands. The coordination geometry of Ag2 is formed by N2, N3, and O3 from two $HPIDC^{2-}$ ligands. The bond lengths of Ag–O are 2.150(2)–2.565(3) Å and the bond lengths of Ag–N range are 2.161(3)–2.139(3) Å. The bond angles of O(N)–Ag–O(N) vary from 71.53(11)° to 170.60(12)°.

One interesting structural feature of **1** is the presence of intramolecular C–H···Ag close interactions. The distances of Ag1···H7 and Ag2···H9 are 2.517(3) and 2.598(4) Å and

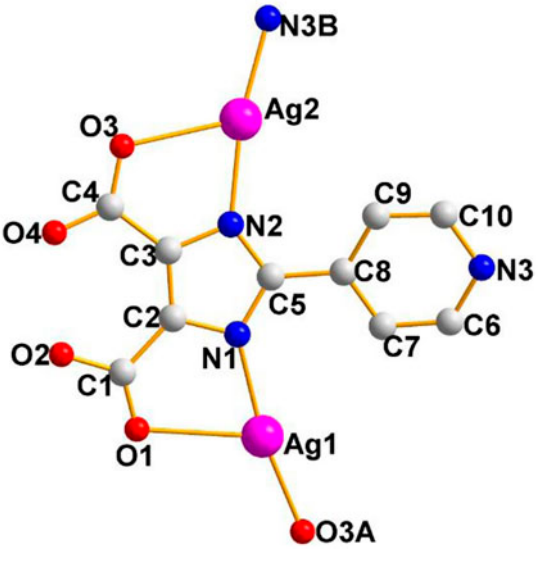

Figure 1(a). View of the asymmetric unit of **1**.

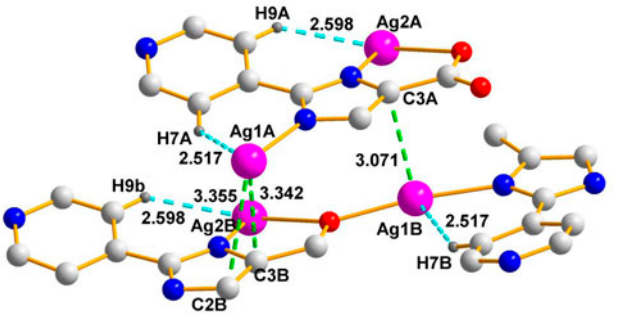

Figure 1(b). View of the intra- and inter-molecular C–H···Ag and Ag···C interactions in **1**.

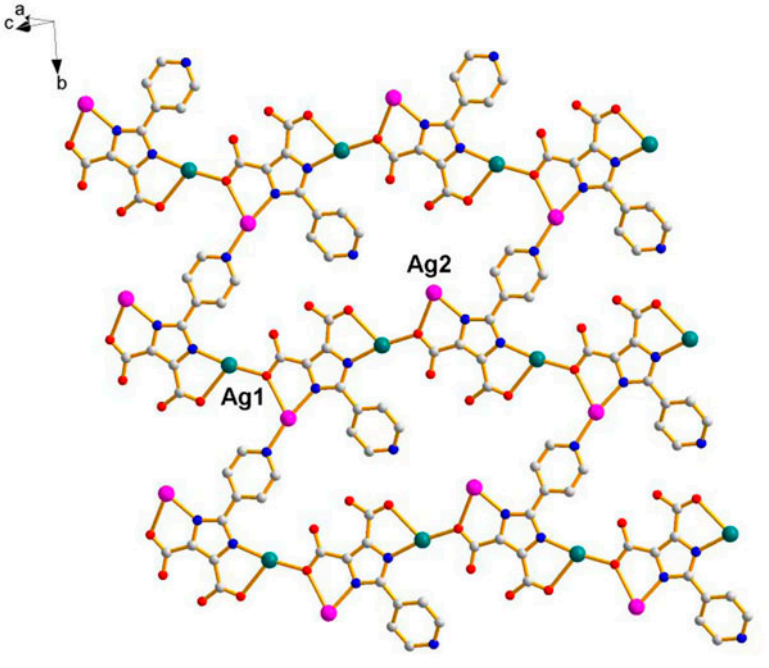

Figure 1(c). View of the 2-D layers of **1**.

angles of C7–H7···Ag1 and C9–H9···Ag2 are 142.00° and 141.66°. These are similar to values for reported Ag(I) complexes [27, 28] and described as weak intermolecular C–H···Ag hydrogen bonding. Meanwhile, the distances of Ag1A···C2B 3.355(46), Ag1A···C3B 3.342(45), and Ag1B···C3A 3.071(45) Å [figure 1(b)] are shorter than the sum of the van der Waals radii of Ag and C (3.42 Å) [29], indicating a weak interaction between Ag(I) and carbon [30–32].

In **1**, the $HPIDC^{2-}$ ligands have the same coordination mode, μ_4-*k*N,O : *k*O : *k*N′,O′ : *k*N″, connecting four Ag(I) ions. As shown in figure 1(c), each $HPIDC^{2-}$ links Ag1 and Ag2 with N and O to form an infinite zigzag chain along the *a*-axis. The angle is 29.18(149)°

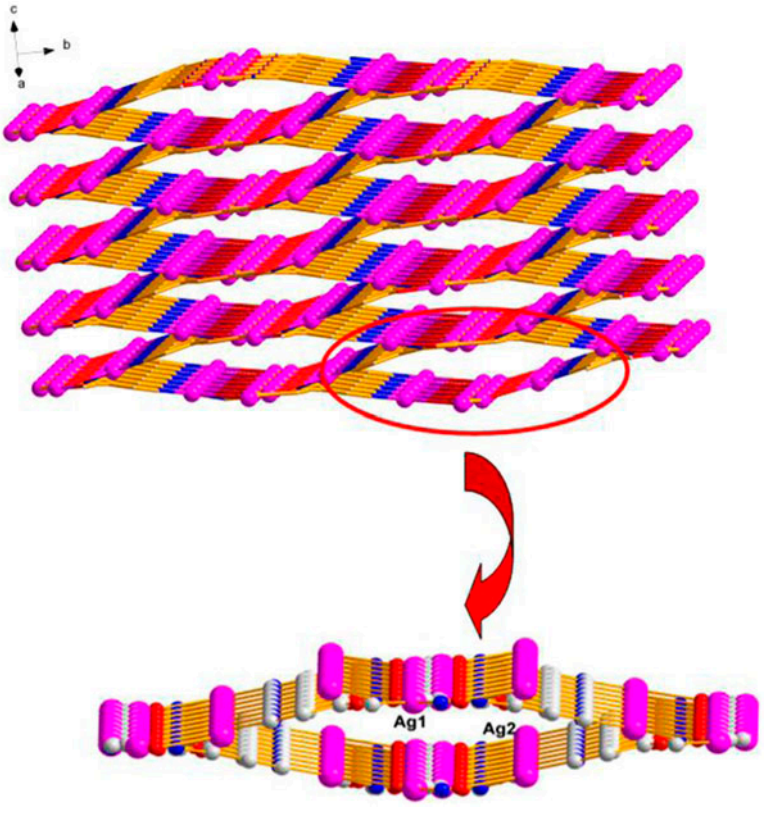

Figure 1(d). View of 3-D framework and the diamond-shaped nano-hole of **1**.

formed by the pyridyl rings of two adjacent ligands hanging on either side of Ag1. Adjacent 1-D zigzag chains are bridged by nitrogen of pyridyl rings from $HPIDC^{2-}$ to form 2-D layers. As the pyridyl rings and imidazole rings have a small dihedral angle of 15.76(159)°, adjacent layers are connected through the pyridyl rings from ligands to generate a 3-D framework [figure 1(d)]. A diamond-shaped nano-hole was formed and diagonals are 5.208 and 10.425 Å [figure 1(d)].

3.3. *Structural description of $[Ag_2(HPIDC)(MBI)]_n$ (2)*

Complex **2** crystallizes in the monoclinic space group P_21/c, with coordination around Ag (I) shown in figure 2(a). The asymmetric unit comprises two Ag(I) (Ag1, Ag2) ions, one $HPIDC^{2-}$, and one MBI. Both Ag1 and Ag2 cations have slightly distorted trilateral environments. The coordinate geometry of Ag1 is completed by O1, N1, and N3A from two $HPIDC^{2-}$ ligands. The coordination sphere of Ag2 also forms by O4, N2, and N4, with N2 from $HPIDC^{2-}$ and N4 from MBI. The Ag-N bond lengths are 2.077(6)–2.141(6) Å, comparable with those observed in related complexes [33–35]. $HPIDC^{2-}$ in **2** also serves as T-shaped 3-connectors similar to in **1**, but adopt a different μ_3-*k*N,O : *k*N′,O′ : *k*N″ coordination connecting three Ag(I) ions in bis-N,O-chelating and one monodentate mode. The

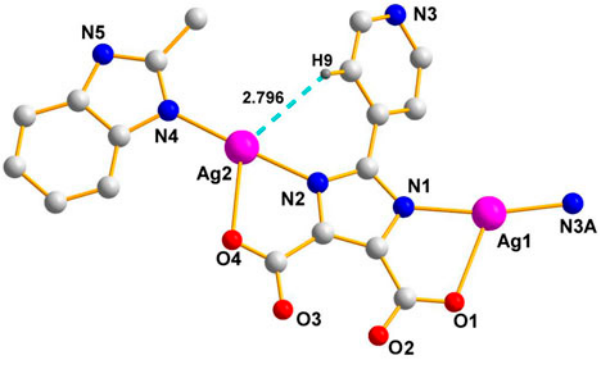

Figure 2(a). View of the asymmetric unit of **2** and the intramolecular C–H···Ag interactions.

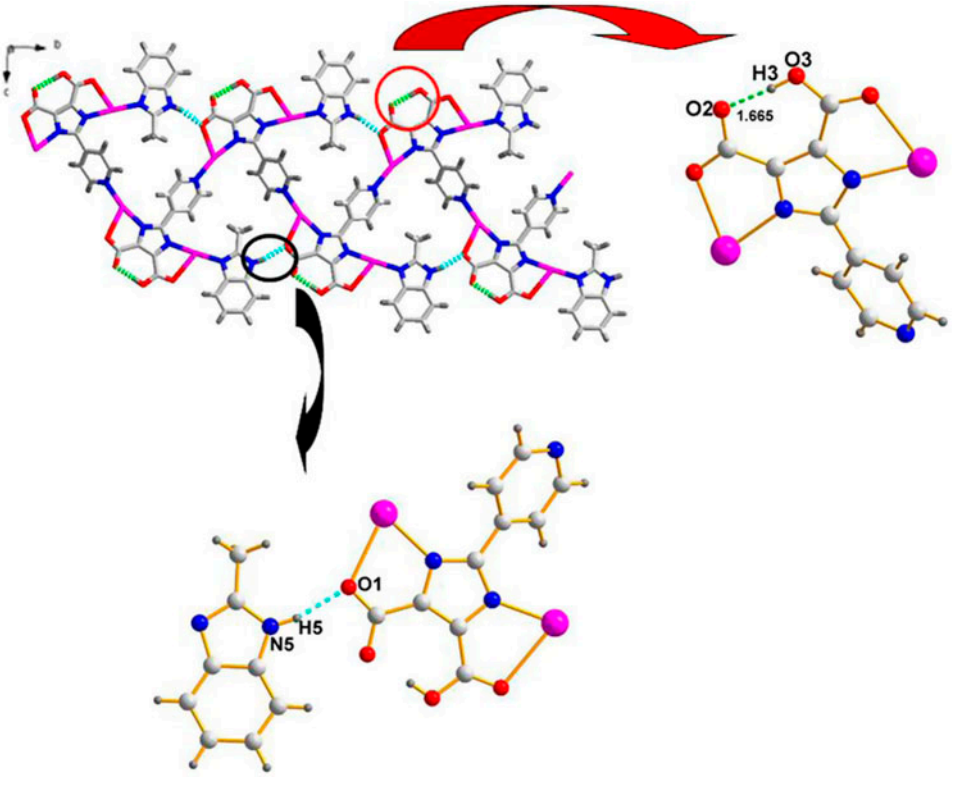

Figure 2(b). View of the 1-D zigzag chain along the *a*-axis and hydrogen bonds in **2**.

imidazole rings and pyridyl rings of $HPIDC^{2-}$ with the dihedral angle of 35.49(265)° are more distorted than in **1**.

There are also C–H···Ag2 close intramolecular interactions between the Ag2 and H9 of pyridyl of H_3PIDC, with Ag2···H9 distance of 2.796(7) Å and Ag2–C9 the distance of 3.338(85) Å and C9–H9···Ag2 angle of 118.25(495)°.

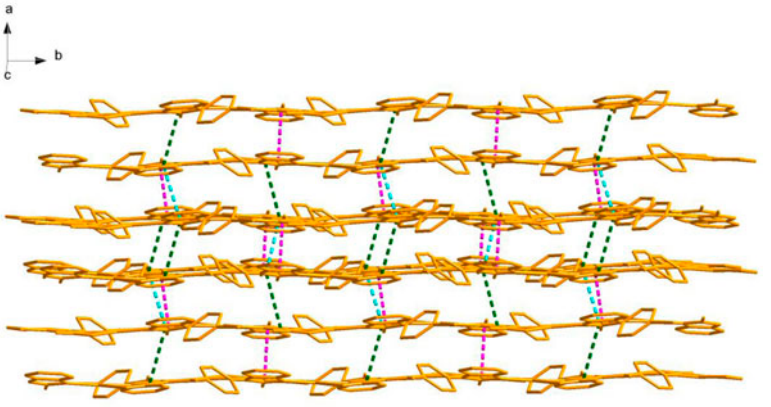

Figure 2(c). View of the 3-D supramolecular framework with $\pi\cdots\pi$ interactions in **2**.

As shown in figure 2(b), $HPIDC^{2-}$ in **2** bridge Ag1 through pyridyl rings in monodentate mode to form a 1-D zigzag chain running along the *a*-axis, and adjacent $HPIDC^{2-}$ ligands in each chain are perpendicular. The intramolecular hydrogen bonds O3–H3···O2 1.665(49) and N5–H5···O1 1.899(1) Å stabilize the 1-D chain; related hydrogen bond data are listed in table 3. Adjacent chains are joined through inter-chain $\pi\cdots\pi$ stacking interactions between imidazole rings of $HPIDC^{2-}$ and MBI with centroid–centroid distances of 3.706(3), 3.782(2), and 3.839(3) Å. Adjacent layers are stacked through $\pi\cdots\pi$ interactions forming a 3-D supramolecular structure [figure 2(c)].

Comparing **2** with **1**, MBI does not change the coordination number of Ag(I), just influenced the coordination mode of H_3PIDC. In **1**, all $HPIDC^{2-}$ ligands have the same coordination, μ_4-*k*N,O : *k*O : *k*N′,O′ : *k*N″, connecting four Ag(I) ions. Complex **2** adopts a different μ_3-*k*N,O : *k*N′,O′ : *k*N″ coordination mode connecting three Ag(I) ions, and the imidazole rings and pyridyl rings of $HPIDC^{2-}$ with dihedral angle of 35.49° are more distorted than in **1** (15.76°).

3.4. *Luminescence*

Considering that coordination complexes with d^{10} metal ions usually exhibit strong luminescence, the solid-state photoluminescence properties of **1**, **2**, H_3PIDC, and MBI have been investigated at their optimal excitation wavelengths at room temperature. UV–Vis strong absorptions at 313 and 286 nm correspond to π–π* transitions of H_3PIDC and MBI, respectively. The shoulder band at 363 nm can be ascribed to inter-ligand charge transfer transition of H_3PIDC whereas the long wavelength absorptions at 408 and 389 nm were produced by metal–ligand charge transfer (^{1}**MLCT**) transitions of **1** and **2**, respectively. As shown in figure 3, emission maxima of H_3PIDC, MBI, **1**, and **2** are located at 466, 314, 588, and 600 nm upon excitation at 363, 286, 408, and 389 nm, respectively. The maxima of **1** and **2** are strongly redshifted, 122 and 134 nm, compared with the free ligand, assigned to **MLCT** emissions [36–38]. The emission intensity of **2** is significantly higher than that of **1**. This different luminescent behavior of **1** and **2** is attributed to their different delocalization environments. In **1**, the imidazole rings and pyridyl rings of the ligand are almost coplanar with dihedral angle of 15.76°. However, in **2,** the dihedral angle between the imidazole rings and pyridyl rings is 35.49°.

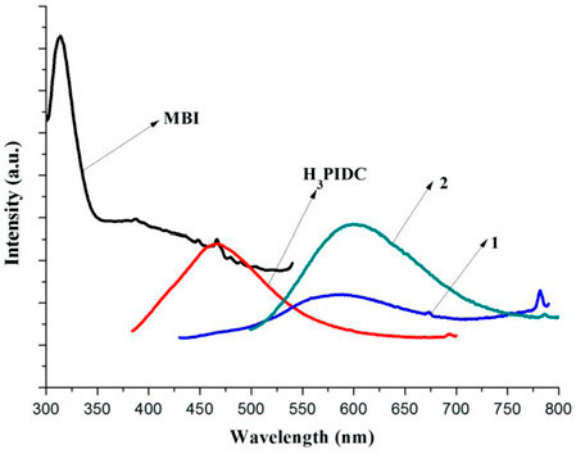

Figure 3. Luminescence curves of H_3PIDC, MBI, **1** and **2**.

3.5. *Thermal analyses*

To study the thermal behavior of **1** and **2**, thermogravimetric analysis was carried out from 20 to 850 °C at a heating rate of 10 °C/min in Ar (Supplementary material, see online supplemental material at http://dx.doi.org/10.1080/00958972.2013.885508)). For **1**, the TGA curve shows that it is stable to 339.2 °C. When the temperature is higher than 339.2 °C, a major weight loss occurs, attributed to collapse of the coordination structure. The remaining weight of 48.04% (Calcd 48.29%) is close to the percentage of the Ag component, indicating that the final gray product is Ag.

For **2**, the TGA curve shows that it is stable to 321.6 °C where weight loss of 62.22% (Calcd 62.74%) from 321.6 to 469.5 °C may be ascribed to decomposition of $HPIDC^{2-}$ and MBI. The remaining weight of 37.78% corresponds to the percentage (37.26%) of Ag. Powdered X-ray diffraction patterns of **1** and **2** are exactly matched with those from single-crystal diffraction patterns (S1 and S2).

4. Conclusion

Two new complexes based on Ag(I) were synthesized under hydrothermal conditions. H_3PIDC possesses different coordination modes in **1** and **2** and the auxiliary MBI exerts influence on the structure of **2**. For **1**, with $HPIDC^{2-}$, a 3-D framework was obtained. In **2**, MBI led to a 1-D zigzag chain and further formed a 3-D supramolecular structure through $\pi\cdots\pi$ interactions. Weak interactions, such as C–H···Ag and Ag···C between the Ag centers and H and C of H_3PIDC, provide additional assembly forces, leading to 3-D supramolecular networks for **1** and **2**. Luminescence measurements show maxima of **1** and **2** are strongly redshifted compared with H_3PIDC; **2** with significantly stronger luminescence is attributed to the second ligand MBI.

Supplementary material

CCDC 937394–937395 contains the supplementary crystallographic data for this article. These data can be obtained free of charge from The Cambridge Crystallographic Data Center via www.ccdc.cam.ac.uk/datarequest/cif.

Funding

This work was supported by the National Natural Science Foundation of China [grant number 21171149].

References

[1] (a) O.M. Yaghi, H. Li, C. Davis, D. Richardson, T.L. Groy. *Acc. Chem. Res.*, **31**, 474 (1998); (b) M. Eddaoudi, D.B. Moler, H. Li, B. Chen, T.M. Reineke, M. O'Keeffe, O.M. Yaghi. *Acc. Chem. Res.*, **34**, 319 (2001); (c) C.N.R. Rao, S. Natarajan, R. Vaidhyanathan. *Angew. Chem., Int. Ed.*, **43**, 1466 (2004); (d) C. Jainak. *Dalton Trans.*, **14**, 2781 (2003); (e) S.M. Kuznicki, V.A. Nair, S. Bell, H.W. Hillhouse, R.M. Jacubinas, C.M. Braunbarth, B.H. Toby, M. Tsapatsis. *Nature*, **412**, 720 (2001).

[2] (a) Y.B. Zhang, W.X. Zhang, F.Y. Feng, J.P. Zhang, X.M. Chen. *Angew. Chem. Int. Ed. Engl.*, **48**, 5287 (2009); (b) Y.G. Huang, B.L. Wu, D.Q. Yuan, Y.Q. Xu, F.L. Jiang, M.C. Hong. *Inorg. Chem.*, **46**, 1171 (2007); (c) J.Y. Wu, M.T. Ding, Y.S. Wen, Y.H. Liu, K.L. Lu. *Chem. Eur. J.*, **15**, 3604 (2009).

[3] (a) L. Pan, X.Y. Huang, J. Li, Y.G. Wu, N.W. Zheng. *Angew. Chem. Int. Ed.*, **39**, 527 (2000); (b) J. Xia, B. Zhao, H.S. Wang, W. Shi, Y. Ma, H.B. Song, P. Cheng, D.Z. Liao, S.P. Yan. *Inorg. Chem.*, **46**, 3405 (2007); (c) X.H. Zhou, Y.H. Peng, X.D. Du, C.F. Wang, J.L. Zuo, X.Z. You. *Cryst. Growth Des.*, **9**, 1028 (2009).

[4] (a) M.L. Tong, S. Kitagawa, H.C. Chang, M. Ohba. *Chem. Commun.*, **4**, 418 (2004); (b) X.J. Gu, D.F. Xue. *CrystEngComm*, **9**, 471 (2007); (c) Z.B. Han, Y.K. He, M.L. Tong, Y.J. Song, X.M. Song, L.G. Yang. *CrystEngComm*, **10**, 1070 (2008); (d) P. Mahata, K.V. Ramya, S. Natarajan. *Chem. Eur. J.*, **14**, 5839 (2008); (e) M. Xue, G.S. Zhu, H. Ding, L. Wu, X.J. Zhao, Z. Jin, S.L. Qiu. *Cryst. Growth Des.*, **9**, 1481 (2009); (f) B.L. Chen, L.B. Wang, Y.Q. Xiao, F.R. Fronczek, M. Xue, Y. Cui, G.D. Qian. *Angew. Chem., Int. Ed.*, **48**, 500 (2009); (g) D. Banerjee, S.J. Kim, L.A. Borkowski, W.Q. Xu, J.B. Parise. *Cryst. Growth Des.*, **10**, 709 (2010).

[5] (a) Y.F. Yue, J. Liang, E.Q. Gao, C.J. Fang, Z.G. Yan, C.H. Yan. *Inorg. Chem.*, **47**, 6115 (2008); (b) W.X. Zhang, W. Xue, J.B. Lin, Y.Z. Zheng, X.M. Chen. *CrystEngComm*, **10**, 1770 (2008); (c) G.F. Liu, L.L. Li, Y.S. Ren, H.X. Li, Z.G. Ren, Y. Zhang, J.P. Lang. *Inorg. Chem. Commun.*, **12**, 563 (2009); (d) W.X. Zhang, W. Xue, Y.Z. Zheng, X.M. Chen. *Chem. Commun.*, **25**, 3804 (2009); (e) G. Yuan, K.Z. Shao, X.L. Wang, Y.Q. Lan, D.Y. Du, Z.M. Su. *CrystEngComm*, **12**, 1147 (2010).

[6] G. Yuan, K.Z. Shao, D.Y. Du, X.L. Wang, Z.M. Su, J.F. Ma. *CrystEngComm*, **14**, 1865 (2012).

[7] L. Sun, G.Z. Li, M.H. Xu, X.J. Li, J.R. Li, H. Deng. *Eur. J. Inorg. Chem.*, **11**, 1764 (2012).

[8] (a) X. Li, B.L. Wu, C.Y. Niu, Y.Y. Niu, H.Y. Zhang. *Cryst. Growth Des.*, **9**, 3423 (2009); (b) X.M. Jing, L.R. Zhang, T.L. Ma, G.H. Li, Y. Yu, Q.S. Huo, M. Eddaoudi, Y.L. Liu. *Cryst. Growth Des.*, **10**, 492 (2010); (c) X.M. Jing, H. Meng, G.H. Li, Y. Yu, Q.S. Huo, M. Eddaoudi, Y.L. Liu. *Cryst. Growth Des.*, **10**, 3489 (2010); (d) G. Yuan, K.Z. Shao, D.Y. Du, X.L. Wang, Z.M. Su, J.F. Ma. *CrystEngComm*, **14**, 1865 (2012); (e) S.R. Zheng, S.L. Cai, Z.Z. Wen, J. Fan, W.G. Zhang. *Polyhedron*, **38**, 190 (2012).

[9] P.J. Steel, C.M. Fitchett. *Coord. Chem. Rev.*, **252**, 990 (2008).

[10] A.N. Khlobystov, A.J. Blake, N.R. Champness, D.A. Lemenovskii, A.G. Majouga, N.V. Zyk, M. Schröder. *Coord. Chem. Rev.*, **222**, 155 (2001).

[11] A.G. Young, L.R. Hanton. *Coord. Chem. Rev.*, **252**, 1346 (2008).

[12] R.S. Zhou, J.F. Song, Y.B. Li, C.Y. Xu, X.F. Yang. *Z. Anorg. Allg. Chem.*, **637**, 251 (2011).

[13] (a) F. Marandi, A. Marandi, M. Ghadermazi, H. Krautscheid, M. Rafiee. *J. Coord. Chem.*, **65**, 1882 (2012); (b) Y.N. Zhang, X. Hai, Y.T. Li, L. Cui, Y.Y. Wang. *J. Coord. Chem.*, **65**, 2724 (2012).

[14] C.Y. Wu, C.S. Lee, S. Pal, W.S. Hwang. *Polyhedron*, **27**, 2681 (2008).

[15] C.S. Liu, P.Q. Chen, Z. Chang, J.J. Wang, L.F. Yan, H.W. Sun, X.H. Bu, Z.Y. Lin, Z.M. Li, S.R. Batten. *Inorg. Chem. Commun.*, **11**, 159 (2008).

[16] Y. Bai, H. Gao, D.B. Dang, X.Y. Guo, B. An, W.L. Shang. *CrystEngComm*, **12**, 1422 (2010).

[17] Y. Bai, G.S. Zheng, D.B. Dang, Y.N. Zheng, P.T. Ma. *Spectrochim. Acta, Part A, Mol. Biomol. Spectrosc.*, **79**, 1338 (2011).

[18] H. Wu, X.W. Dong, H.Y. Liu, J.F. Ma, Y.Y. Liu, Y.Y. Liu, J. Yang. *Inorg. Chim. Acta*, **19**, 373 (2011).

[19] (a) J.A. Zhao, J.Y. Hu, Y. Bai, S.F. Chen, S.S. Li. *J. Coord. Chem.*, **65**, 3216 (2012); (b) J.J. Wang, L.J. Gao, P.X. Cao, Y.P. Wu, F. Fu, M.L. Zhang, Y.X. Ren, X.Y. Hou. *J. Coord. Chem.*, **65**, 3614 (2012); (c) M. Hakimi, K. Moeini, Z. Mardani, E. Schuh, F. Mohr. *J. Coord. Chem.*, **66**, 1129 (2013).

[20] X. Yu, Chi, H.P. Dai, S.M. Li, J. Jin, S.Y. Niu, G.N. Zhang. *Spectrochim. Acta, Part A, Mol. Biomol. Spectrosc.*, **106**, 203 (2013).

[21] J. Qu, Y.L. Yi, Y.M. Hu, W.T. Chen, H.L. Gao, J.Z. Cui, B. Zhai. *J. Coord. Chem.*, **65**, 3740 (2012).

[22] J.A. Zhao, S.S. Li, S.F. Chen, Y. Bai, J.Y. Hu. *J. Coord. Chem.*, **65**, 1201 (2012).

[23] Q.Q. Guo, C.Y. Xu, D.D. Zhao, Y.Y. Jia, X.J. Wang, H.W. Hou, Y.T. Fan. *Z. Anorg. Allg. Chem.*, **638**, 868 (2012).
[24] T. Sun, J.P. Ma, R.Q. Huang, Y.B. Dong. *Acta Crystallogr. Sect. E: Struct. Rep. Online*, **62**, o2751 (2006).
[25] G.M. Sheldrick, *SHELXL-97, Program for the Refinement of Crystal Structures*, p. 3211, University of Göttingen, Germany (1997).
[26] N. Kazuo. *Infrared and Raman Spectra of Inorganic and Coordination Compounds, Part B: Applications in Coordination, Organometallic, and Bioinorganic Chemistry*, p. 64, Marquette University, Wiley, Hoboken, NJ (2009).
[27] C.S. Liu, Z. Chang, J.J. Wang, L.F. Yan, X.H. Bu, S.R. Batten. *Inorg. Chem. Commun.*, **11**, 889 (2008).
[28] D. Braga, F. Grepioni, E. Tedesco, K. Biradha, G.R. Desiraju. *Organometallics*, **16**, 1846 (1997).
[29] V.T. Yilmaz, S. Hamamci, C. Kazak. *J. Organomet. Chem.*, **693**, 3885 (2008).
[30] T.S. Thakur, G.R. Desiraju. *Chem. Commun.*, **5**, 552 (2006).
[31] C.S. Liu, P.Q. Chen, E.C. Yang, J.L. Tian, X.H. Bu, Z.M. Li, H.W. Sun, Z.Y. Lin. *Inorg. Chem.*, **45**, 5812 (2006).
[32] O.Z. Yeşilel, G. Günay, O. Büyükgüngör. *Polyhedron*, **30**, 364 (2011).
[33] W.G. Lu, L. Jiang, X.L. Feng, T.B. Lu. *Inorg. Chem.*, **48**, 6997 (2009).
[34] X. Feng, J.S. Zhao, B. Liu, L.Y. Wang, S.W. Ng, G. Zhang, J.G. Wang, X.G. Shi, Y.Y. Liu. *Cryst. Growth Des.*, **10**, 1399 (2010).
[35] Y.Q. Sun, J. Zhang, G.Y. Yang. *Chem. Commun.*, **45**, 4700 (2006).
[36] C.L. Chen, B.S. Kang, C.Y. Su. *Aust. J. Chem.*, **59**, 3 (2006).
[37] (a) H.L. Hsiao, C.J. Wu, W. Hsu, C.W. Yeh, M.Y. Xie, W.J. Huang, J.D. Chen. *CrystEngComm*, **14**, 8143 (2012); (b) A. Vogler, H. Kunkely. *Top. Curr. Chem.*, **213**, 143 (2001).
[38] J.P. Zhang, Y.Y. Lin, X.C. Huang, X.M. Chen. *J. Am. Chem. Soc.*, **127**, 5495 (2005).